Human Molecular Genetics, 2009, Vol. 18, No. 23 ***4478–4491***
doi:10.1093/hmg/ddp407
Advance Access published on August 21, 2009

Lowe syndrome patient fibroblasts display Ocrl1-specific cell migration defects that cannot be rescued by the homologous Inpp5b phosphatase

Brian G. Coon[1,2], Debarati Mukherjee[1,2], Claudia B. Hanna[1,2], David J. Riese II[2], Martin Lowe[3] and R. Claudio Aguilar[1,2,*]

[1]Department of Biological Sciences and [2]Purdue Center for Cancer Research, Purdue University, West Lafayette, IN 47907, USA and [3]Faculty of Life Sciences, University of Manchester, Manchester M13 9PT, UK

Received May 20, 2009; Revised July 24, 2009; Accepted August 20, 2009

The Lowe syndrome (LS) is a life-threatening, developmental disease characterized by mental retardation, cataracts and renal failure. Although this human illness has been linked to defective function of the phosphatidylinositol 5-phosphatase, Ocrl1 (Oculo-Cerebro-Renal syndrome of Lowe protein 1), the mechanism by which this enzyme deficiency triggers the disease is not clear. Ocrl1 is known to localize mainly to the Golgi apparatus and endosomes, however it translocates to plasma membrane ruffles upon cell stimulation with growth factors. The functional implications of this inducible translocation to the plasma membrane are presently unknown. Here we show that Ocrl1 is required for proper cell migration, spreading and fluid-phase uptake in both established cell lines and human dermal fibroblasts. We found that primary fibroblasts from two patients diagnosed with LS displayed defects in these cellular processes. Importantly, these abnormalities were suppressed by expressing wild-type Ocrl1 but not by a phosphatase-deficient mutant. Interestingly, the homologous human PI-5-phosphatase, Inpp5b, was unable to complement the Ocrl1-dependent cell migration defect. Further, Ocrl1 variants that cannot bind the endocytic adaptor AP2 or clathrin, like Inpp5b, were less apt to rescue the migration phenotype. However, no defect in membrane recruitment of AP2/clathrin or in transferrin endocytosis by patient cells was detected. Collectively, our results suggest that Ocrl1, but not Inpp5b, is involved in ruffle-mediated membrane remodeling. Our results provide new elements for understanding how Ocrl1 deficiency leads to the abnormalities associated with the LS.

INTRODUCTION

The Oculo-Cerebro-Renal syndrome of Lowe (OCRL) is a recessive, X-linked genetic disease characterized by the presence of congenital cataracts, mental retardation and renal dysfunction (1–3). This disorder is associated with abnormal function of the Inositol 5-phosphatase (EC 3.1.3.36) Ocrl1, responsible for the hydrolysis of Phosphatidyl Inositol (PtdIns) 5-phosphates including PtdIns (4,5) bi-phosphate (PIP_2) (4–7), a plasma membrane-enriched phospholipid. Most *OCRL1* gene mutations found in Lowe syndrome (LS) patients either lead to absence of the gene product or to deficient phosphatase activity (4,8). Indeed, cells of LS patients frequently possess higher intracellular levels of PIP_2 than do normal cells (6,9). However, it is still uncertain how this lipid imbalance, or the lack of Ocrl1, causes the developmental abnormalities that characterize the disease.

Although Ocrl1 primarily localizes to the Golgi apparatus (1,10,11) and early endosomes (12–15), the pioneering work of Faucherre *et al*. (9) demonstrates that this protein also translocates to membrane ruffles upon stimulation of growth factor receptors. Therefore, we and others (9) have speculated that this protein might be relevant to processes that require plasma membrane remodeling, such as cell migration.

Here we report a novel cellular phenotype associated with LS. Relative to fibroblasts from normal individuals, LS

*To whom correspondence should be addressed. +1 7654963547; Fax: +1 7654961496; Email: claudio@purdue.edu

fibroblasts are impaired for cell migration. Other processes requiring extensive membrane remodeling, such as cell spreading and fluid-phase uptake, are also affected in LS cells. These defects are specific for a lack of Ocrl1 function and they cannot be rescued by expression of the homologous phosphatase Inpp5b.

We speculate that these novel phenotypes would have consequences on aspects of embryo development and cell physiology contributing to LS pathology.

RESULTS

Ocrl1 localizes to plasma membrane ruffles of migrating cells

Faucherre *et al*. (9) demonstrated that upon stimulation with growth factors, Ocrl1 localizes to plasma membrane ruffles in COS-7 cells; therefore, we hypothesized that this protein plays a role in cellular processes that require plasma membrane remodeling, such as cell migration. Indeed, we observed that in addition to Golgi localization, migrating HeLa and HT1080 human cells and NIH3T3 murine fibroblasts accumulated GFP-Ocrl1 in membrane ruffles (Fig. 1).

Time-lapse microscopy indicated that GFP-Ocrl1 was dynamically recruited to the leading edge of migrating cells (Supplementary Material, Movie S1 and Fig. S1). We also observed dynamic puncta and tubular structures (Supplementary Material, Movies S1 and S2) previously noted by other investigators (14). Moreover, circular structures decorated with GFP-Ocrl1 appeared to be assembled in ruffles and moved towards the cell central region (Supplementary Material, Movies S1 and S2, and Fig. S1). Since these structures also contained clathrin (that partially co-localized with Ocrl1—Supplementary Material, Fig. S1), we speculated that they might be endocytic in nature. In fact, clathrin is a known Ocrl1-interaction partner (13,14).

Ocrl1 function is required for proper cell migration

Since Ocrl1 was enriched in membrane ruffles at the leading edge of migrating cells (Fig. 1), we tested whether Ocrl1 plays an active role in cell migration. Therefore, the ability of Ocrl1 knock-down cells to migrate through transwell filters was examined (Fig. 2A and B). Knocking down Ocrl1 expression significantly impaired migration of human HeLa and mouse NIH3T3 cells relative to control cells (Fig. 2C and D). Importantly, this phenotype was specifically linked to Ocrl1-deficiency as it was rescued by expression of a siRNA-resistant GFP-Ocrl1 construct (Fig. 2D).

LS cells are deficient for cell migration

We reasoned that if Ocrl1 is required for proper cell migration, then cells from LS patients should also display defects in this process. We first characterized fibroblasts from two different patients diagnosed with Lowe syndrome: LS1 and LS2. Western blotting with specific antibodies indicated that these fibroblasts did not express detectable levels of Ocrl1 but displayed significant amounts of the homologous phosphatase Inpp5b (Fig. 3A).

Next, we assessed migration of LS and control cells using the transwell assay. We transfected LS and normal fibroblast with GFP, GFP-Ocrl1^{WT} or GFP-Ocrl1^{H507R} and assayed the resulting transfectants for migration in transwells. Figure 3B reveals that both LS cell migrated less than normal cells in a transwell assay. Moreover, the defect in migration of LS cells was rescued by expression of WT human Ocrl1-GFP (Fig. 3B). However, expression of a phosphatase-deficient Ocrl1 variant (Ocrl1^{H507R}) identified in another LS patient (16) was unable to rescue the defect in migration of LS cells (Fig. 3B). These data support the idea that genetic lesions leading to LS, either by causing absence of Ocrl1 expression (LS1 and LS2; Fig. 3A) or inactivation of its phosphatase activity (Ocrl1^{H507R}; Fig. 3B), affect patients' cells ability to migrate. Levels of expression of all GFP-fusion constructs were comparable (Supplementary Material, Fig. S2).

Further, these results were confirmed using a 'wound-healing' migration assay (Fig. 4). LS cells exhibited a significantly lower extent of migration towards a newly generated cell-free space than did normal fibroblasts (Fig. 4A and B).

LS cell migration defect does not involve Golgi polarization abnormalities and it is independent of the nature of the migration stimuli

Since Ocrl1 mainly localizes at the Golgi apparatus (1,10,11) and this organelle is oriented towards the leading edge during cell migration (17), we tested whether reduced Ocrl1 expression is associated with abnormalities in the polarization of the Golgi apparatus. 'Wound-healing' assays on LS versus normal cells were performed, followed by fixation and staining of nuclei and Golgi apparatus. The extent of polarization of the Golgi apparatus during migration was assessed by determination of Θ, the angle between the nucleus-Golgi and the nucleus-leading edge axes (Fig. 4C). Migrating LS and control cells were stained with DAPI, rhodamine–phalloidin and by immunofluorescence using an antibody against the *trans*-Golgi network resident protein TGN46 (Fig. 4D). Our results revealed that the polarity of the Golgi apparatus was not significantly altered in LS cells (Fig. 4D and E).

We next asked whether the deficit in migration displayed by the LS cells involved changes in the response to haptotactic and/or chemotatic stimuli. Since different motility modes rely on different subsets of cell surface and signaling molecules (18,19), these experiments had the potential to provide information about specific signaling pathways affected in LS cells. We used modified versions of the transwell migration assay to compare the responses of LS and normal cells to hapto and chemotactic stimuli (Fig. 5). LS cells displayed abnormal responses to both types of stimuli (Fig. 5). These results suggested that the deficiency in Ocrl1 activity in LS cells caused basic cell migration defects that did not depend on specific sensing/signaling mechanisms.

Cell migration defects of LS fibroblasts cannot be rescued by transfection of the Ocrl1–homologous phosphatase Inpp5b

Ocrl1 and the homologous phosphatase Inpp5b show common domain composition (20), share interaction partners

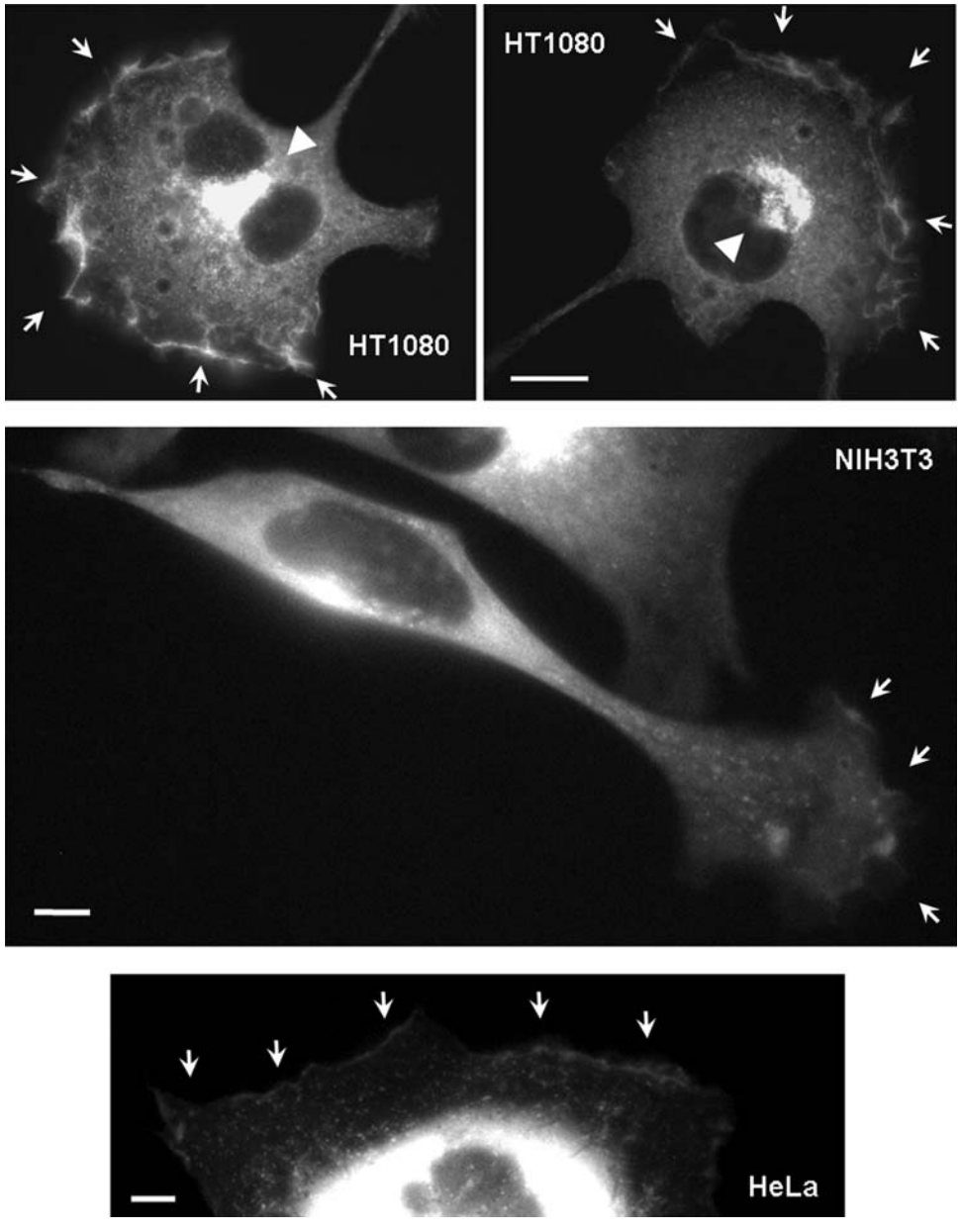

Figure 1. Ocrl1 localizes to membrane ruffles of migrating cells. HT1080 and HeLa cells expressing GFP-Ocrl1 were serum-starved (0.1% FBS) for at least 8 h, stimulated with 10% FBS for 15 min, fixed and imaged. NIH3T3 cells were plated on fibronectin-coated imaging chambers and allowed to migrate for 3 h before live imaging (See Supplementary Material, Movie S1). Arrows point to membrane ruffle structures decorated with GFP-Ocrl1. Arrowheads highlight polarized Golgi apparatus. Scale bars: 10 μm (HT1080) and 5 μm.

(11,12,15,20,21) and exhibit functional overlap (22). In fact, although *Ocrl1* knock-out mice do not display typical symptoms of LS (22), the double *Ocrl1/Inpp5b* knock-out results in embryonic lethality (22). These findings clearly indicate an essential functional redundancy between these two enzymes.

Fibroblasts from LS1 and LS2 patients expressed similar levels of Inpp5b compared with control cells (Fig. 3A). Yet, LS cells displayed Ocrl1-dependent deficiencies in cell migration (Fig. 3B). Thus, we postulated that either: (i) the endogenous Inpp5b expression in LS cells is inadequate to sustain cell migration in the absence of Ocrl1; or that (ii) Inpp5b cannot fulfill the role of Ocrl1 in cell migration. If the first hypothesis is valid then supplementing the endogenous levels by transfecting human Inpp5b constructs should rescue the defect in cell migration exhibited by LS cells. If alternative (ii) is true, then exogenous Inpp5b should not rescue the defect in migration exhibited by the LS cells.

Expression of GFP-Ocrl1 rescued the deficiency in cell migration displayed by the LS cells. In contrast, expression of GFP-Inpp5b did not rescue this defect (Fig. 6A). Similar results were obtained when using a Flag-tagged version of Inpp5b (data not shown), suggesting that the inability of GFP-Inpp5b to rescue the migration deficit displayed by LS cells was not due to interference of Inpp5b function by the

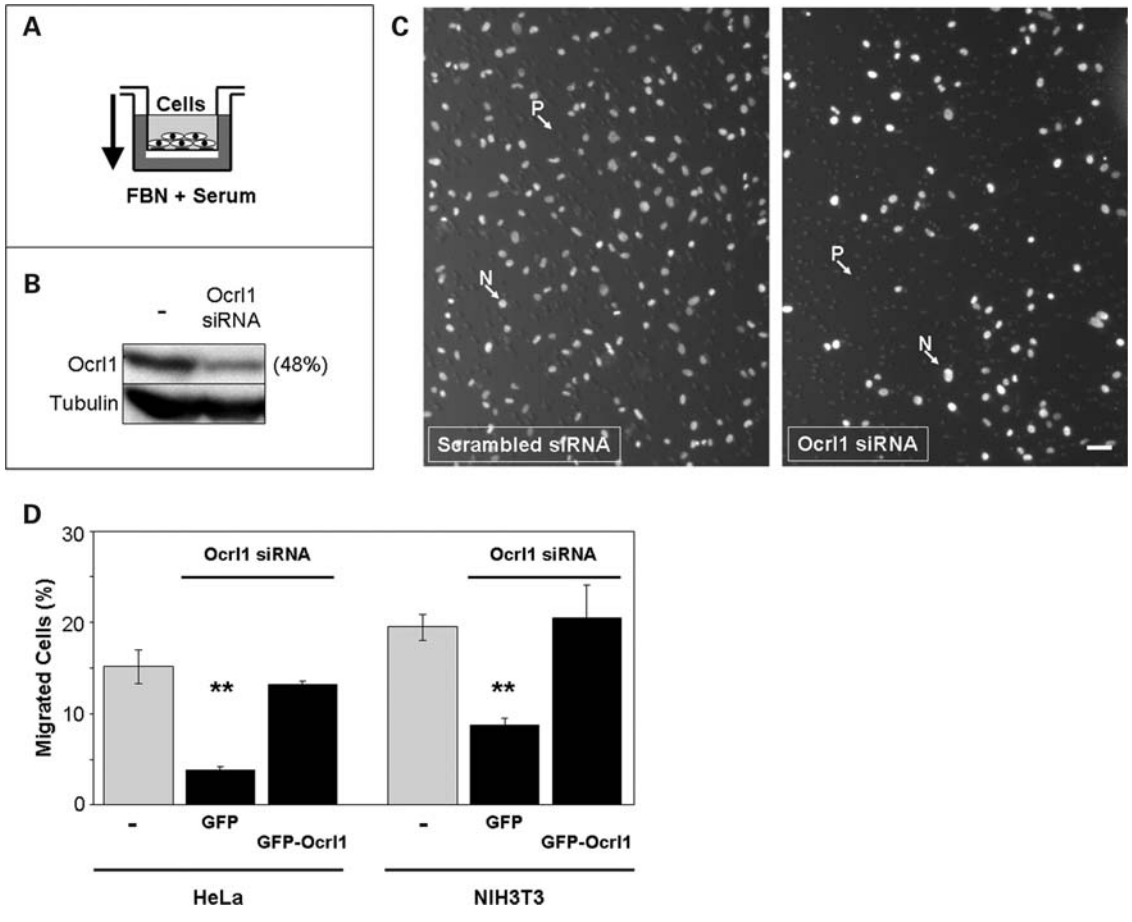

Figure 2. Ocrl1 is required for proper cell migration. (**A**) Cartoon depicts the experimental setup of a transwell migration assay. Cells seeded in the upper chamber (transwell) migrate towards the lower chamber through 8 μm pores following a gradient of serum and fibronectin (FBN). (**B**) Cells were knocked-down for Ocrl1 and the extent of the depletion was controlled by investigating the presence of Ocrl1 in whole cell lysates by western blotting with a specific antibody. Example shows results obtain with HeLa cells treated with Ocrl1 siRNA or Scrambled RNA oligos. Band intensity was determined by densitometry and the results expressed as percentage of the scrambled RNA-treated sample. The presence of tubulin was also determined and used as loading control. (**C**) Cells treated with Ocrl1 siRNA or scrambled oligos were allowed to migrate in an experimental setup as shown in (A). Cells remaining in the upper chamber were removed by swabbing with a q-tip and the migrated cells (filter lower face) were fixed with 3% formaldehyde and visualized by DAPI staining and imaged. N: Nuclei; P: 8 μm pore. Scale bar: 50 μm. (**D**) HeLa and NIH3T3 cells were knocked down using siRNA against human and mouse Ocrl1, respectively, scrambled siRNA or mock-treated. Following transfection with GFP or siRNA-resistant GFP-Ocrl1, cells were assayed for migration in transwells as described under Materials and Methods. Values represent the mean ± SD of at least three independent determinations. Statistical significance was estimated using paired *t*-tests with a correction for significant threshold according to the number of test performed ($\alpha = 0.05/2 = 0.025$). $^{**}P < 0.025$.

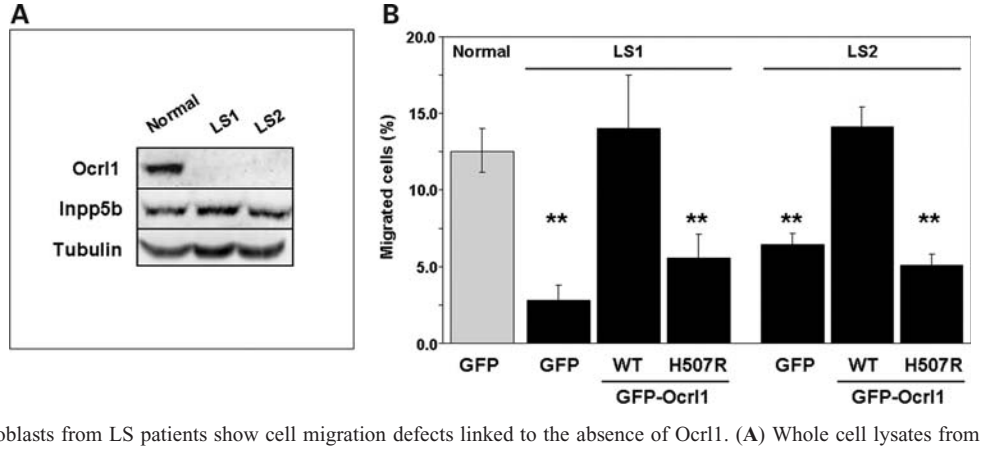

Figure 3. Dermal fibroblasts from LS patients show cell migration defects linked to the absence of Ocrl1. (**A**) Whole cell lysates from LS patient and normal control cells were resolved by SDS–PAGE and the presence of Ocrl1 and Inpp5b was investigated by western blotting with specific antibodies. Tubulin was used as a loading control. (**B**) Normal and LS fibroblasts transfected with the indicated cDNAs were assayed for migration in transwells as described under Materials and Methods. Values represent the mean ± SD of at least three independent determinations. Statistical significance was estimated using paired *t*-tests with a correction for significant threshold according to the number of test performed ($\alpha = 0.05/3 = 0.017$). $^{**}P < 0.017$.

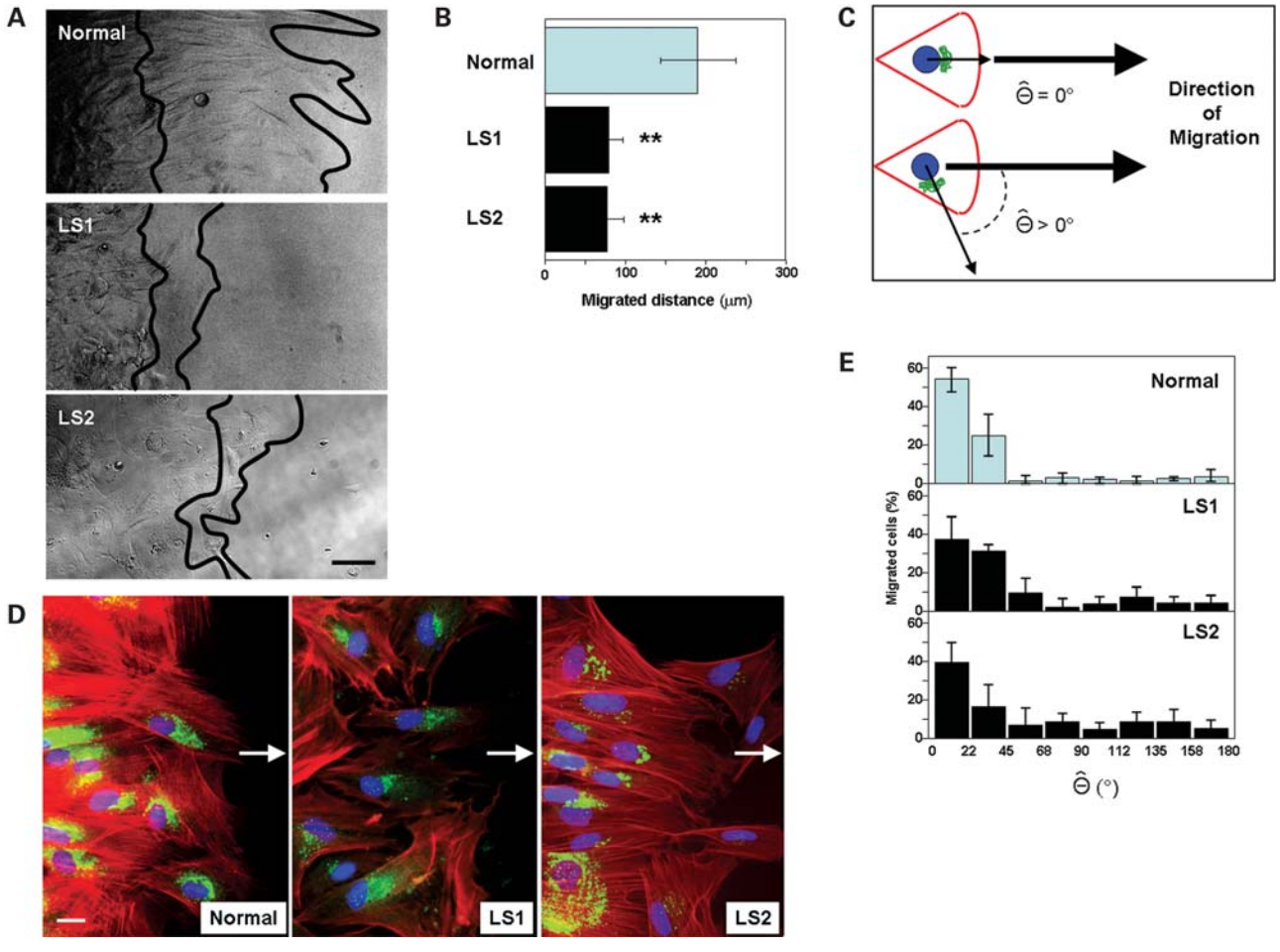

Figure 4. LS fibroblast cell migration defects do not involve Golgi polarization abnormalities. (**A**) Normal and LS patient fibroblasts seeded to confluency were allowed to migrate towards a newly generated cell-free space (see Materials and Methods for details). Lines indicate position of the front of cells after 0 (left) and 12 h (right) of migration. Scale bar: 50 μm. (**B**) The cell-free ('wound') distance covered by migratory cells was measured using ImageJ software. Values represent the mean ± SD of three to five experiments. Statistical significance was estimated using paired *t*-tests with a correction for significant threshold according to the number of test performed ($\alpha = 0.05/2 = 0.025$). $^{**}P < 0.025$. (**C**) As depicted in the cartoon, the Θ angle value is proportional to the lack of co-linearity between the nucleus-Golgi and the nucleus-direction of migration axes. (**D**) Cells migrating towards a cell-free space (arrow) were fixed, permeabilized and stained using DAPI (blue), rhodamine-phalloidin (red) and an anti-TGN46 antibody (followed by a FITC-conjugated secondary antibody, green) to reveal the relative positions of the nuclei, actin cytoskeleton and *trans*-Golgi network, respectively. Scale bar: 20 μm. (**E**) Plots show the Θ distribution for Normal, LS1 and LS2 migratory cells (i.e. at the 'wound' front).

GFP moiety. Levels of expression of the GFP-fusions were comparable (Supplementary Material, Fig. S2). Finally, knocking down expression of Inpp5b with specific siRNAs did not affect the migration of HeLa cells in transwells (Fig. 6B). Taken together, these results strongly suggest that the functional overlap between Ocrl1 and Inpp5b does not extend to cell migration.

The ability of Ocrl1 to efficiently localize to membrane ruffles and to sustain cell migration requires Ocrl1-specific clathrin- and AP2-binding determinants

Ocrl1and Inpp5b display significant sequence homology and equivalent domain composition (Fig. 7A), yet only Ocrl1 rescued the defect in migration displayed by LS cells (Fig. 6A). Therefore, we reasoned that the limited regions of dissimilarity between Ocrl1 and Inpp5b should be responsible for their differential ability to sustain fibroblast migration. As shown in Figure 7A, the differences between these proteins are concentrated near the amino terminus, where a PH domain has been recently described (23). This region of Ocrl1 contains only a few recognizable sequence motifs, including putative binding sites for the endocytic proteins clathrin and AP2 (11,13,14). A second putative clathrin-binding motif is found just preceding the inactive RhoGAP domain of Ocrl1 (13) (Fig. 7A). Furthermore, partial co-localization of Ocrl1 with clathrin and AP2 has been reported (11–14) and we have confirmed and extended these observations to membrane ruffles (Supplementary Material, Movie S2 and Fig. S1). Thus, we deleted the Clathrin-Binding and AP2-Binding Motifs (CBM and ABM, respectively; Fig. 7A) of Ocrl1 and tested whether these mutated proteins rescued the defect in cell migration displayed by LS fibroblasts. Results shown in Figure 7B indicate that deletion of the CBM and ABM motifs of Ocrl1 disrupted the ability of Ocrl1 to rescue the defect in cell migration displayed by LS fibroblasts.

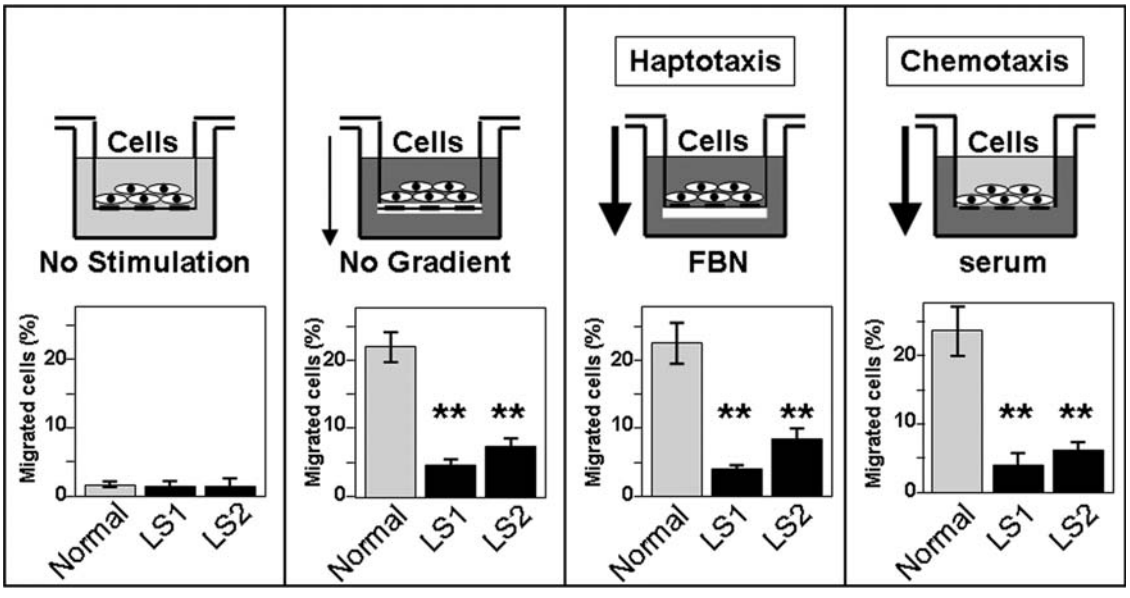

Figure 5. Dermal fibroblast from LS patients show cell migration defects independent of the nature of the migration stimuli. Normal and patient fibroblasts were allowed to migrate towards a gradient of fibronectin (FBN-Haptotaxis) or serum (Chemotaxis) and in the absence of gradient or stimulation. Schemes depict the different modalities of migration in transwell assays. Values represent the mean ± SD of independent determinations. Statistical significance was estimated using paired *t*-tests with a correction for significant threshold according to the number of test performed ($\alpha = 0.05/2 = 0.025$). $^{**}P < 0.025$.

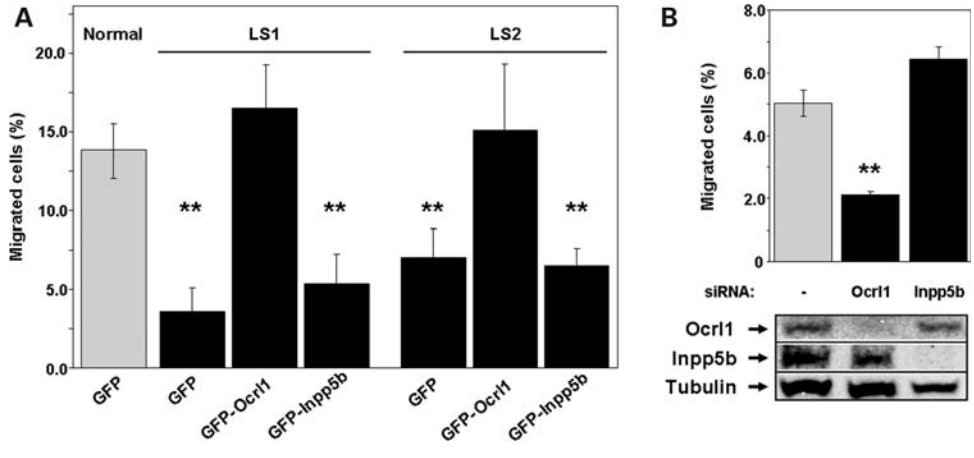

Figure 6. Cell migration depends on Ocrl1 but not on Inpp5b functional status. (**A**) Normal and LS fibroblasts transfected with the indicated cDNAs were assayed for migration in transwells as described under Materials and Methods. Values represent the mean ± SD of at least three independent determinations. Statistical significance was estimated using paired *t*-tests with a correction for significant threshold according to the number of test performed ($\alpha = 0.05/3 = 0.017$). $^{**}P < 0.017$. (**B**) HeLa cells were knocked-down using siRNA against human Ocrl1 and Inpp5b, respectively, or mock-treated. Cells were assayed for migration in transwells as described under Materials and Methods. Values represent the mean ± SD of at least three independent determinations. Statistical significance was estimated using paired *t*-tests with a correction for significant threshold according to the number of test performed ($\alpha = 0.05/2 = 0.025$). $^{**}P < 0.025$. Knock-down efficiency was controlled by western blotting with specific antibodies. Tubulin was used as loading control.

We speculated that the importance of the Ocrl1-clathrin and Ocrl1-AP2 interactions to cell migration could be explained by two mutually exclusive mechanisms: (i) since endocytosis plays an important role in cell migration (24–27), Ocrl1 may be required for binding and recruitment of clathrin/AP2 to nascent endocytic sites. However, it is known that both clathrin and AP2 are 'hubs' in the protein–protein interaction network involved in endocytosis; in other words, they bind and are recognized by most endocytic proteins (28). Therefore, it is unlikely that lack of Ocrl1 would lead to a significant defect in clathrin and AP2 recruitment to endocytic sites that would explain the observed migration abnormalities.

(ii) It is also possible that binding to AP2 and clathrin is important for Ocrl1 recruitment to specific sites within membranes. Once in place, Ocrl1 would function either by exerting its phosphatase activity (contributing to endocytic site dynamics) or via a yet-to-be-established mechanism.

The first hypothesis predicts that in LS cells, clathrin/AP2 structures will be absent or at least abnormal, thereby leading to defects in endocytosis. It is also possible that

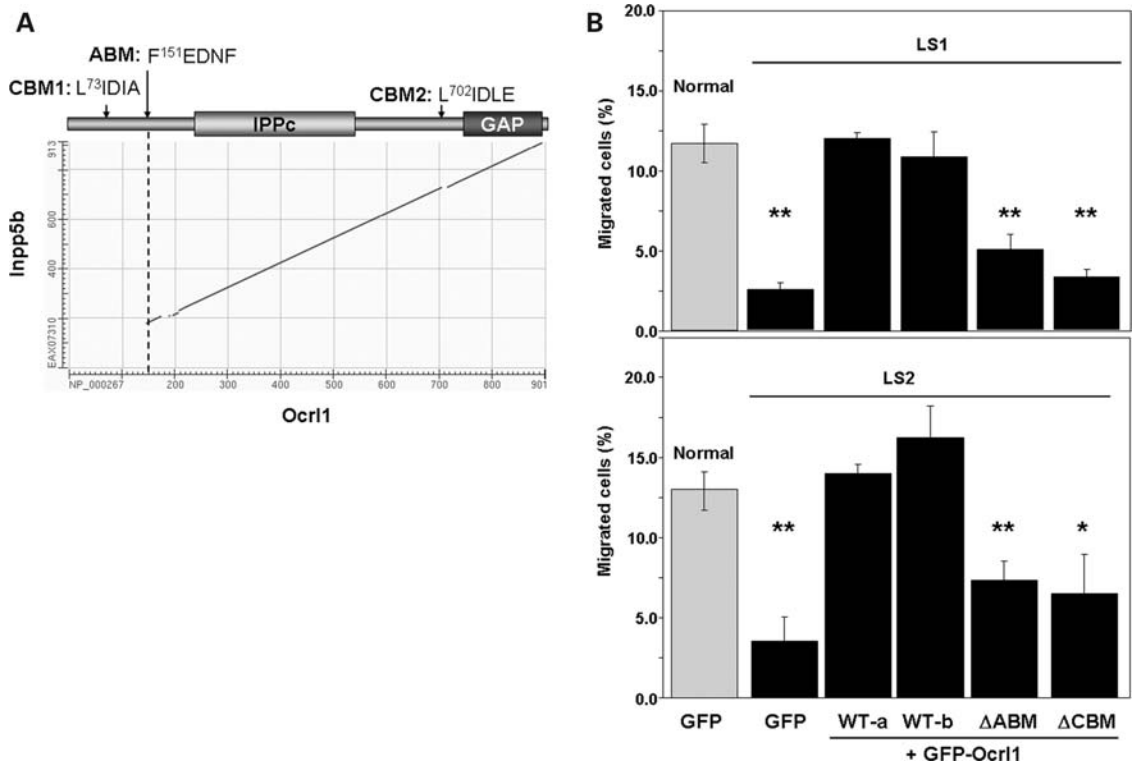

Figure 7. Ocrl1-specific clathrin- and AP2-binding motifs are required for proper migration of dermal fibroblasts. (**A**) Plot shows homology between the protein sequences of Inpp5b (EAX07310) and Ocrl1 (NP_000267) as computed by BLASTP (NCBI, NIH). Cartoon highlights the positions of clathrin- (CBM1 and 2) and AP2-binding (ABM) motifs. IPPc: Inositol PolyPhosphatase catalytic domain; GAP: GTPase Activating Protein-like domain. (**B**) Normal and LS fibroblasts transfected with the indicated cDNAs were assayed for migration in transwells as described under Materials and Methods. WT-a: Ocrl1 wild-type, isoform a; WT-b: Ocrl1 wild-type, isoform b. Values represent the mean ± SD of at least three independent determinations. Statistical significance was estimated using paired *t*-tests with a correction for significant threshold according to the number of test performed ($\alpha = 0.05/5 = 0.01$). $^{**}P < 0.01$; $^{*}P < 0.015$.

elevated or static pools of PIP_2 due to the reduced expression of Ocrl1 in LS cells may lead to abnormalities in the recruitment or function of the endocytic machinery. The second hypothesis predicts that mutated versions of Ocrl1 lacking clathrin- and/or AP2-binding motifs would fail to localize to appropriate, specific subcellular regions.

We evaluated these two hypotheses by first comparing the status of the AP2/clathrin-positive structures in LS versus normal cells. Immunofluorescence microscopy revealed that LS cells displayed clathrin and AP2 localization indistinguishable from normal controls (Supplementary Material, Fig. S3A; data not shown). Indeed, and in agreement with previous reports (29), migrating LS cells exhibited polarized clathrin and AP2 distribution at the leading edge. Since transferrin (Tf) receptor is internalized exclusively via an AP2- and clathrin-dependent mechanism (30,31), we analyzed the uptake of FITC-tagged transferrin (FITC-Tf) by LS and normal cells. The results indicate that internalization of FITC-Tf proceeded in a very similar manner in LS and control cells (Supplementary Material, Fig. S3B and C). We also found no difference between LS and controls cells for the uptake of epidermal growth factor labeled with tetramethylrhodamine or ^{125}I (data not shown). Therefore, our results do not support a major role for Ocrl1 in the recruitment of clathrin/AP2 or in receptor internalization. Further, we also found no significant difference between normal and LS cells for β1-integrin internalization (data not shown).

Since Ocrl1 did not seem to be required for AP2 or clathrin function, we tested our second mechanistic hypothesis; i.e. if the interaction with these endocytic proteins was required for the correct subcellular localization of Ocrl1. It has been clearly established that Inpp5b and Ocrl1 differ in their intracellular distribution (32). Inpp5b is enriched in the ER/*cis*-Golgi transition region, whereas Ocrl1 accumulates in the *trans*-Golgi/endosome/plasma membrane compartments (32). Further, we established that although both GFP-Ocrl1 and GFP-Inpp5b showed broad and partially overlapping intracellular distributions, GFP-Ocrl1 exhibited greater accumulation in membrane ruffles than GFP-Inpp5b (Fig. 8A).

Although it is known that multiple determinants participate in Ocrl1 localization (including the RhoGAP domain and Rab-binding sites; 9,15), we speculated that clathrin and AP2 binding somehow contributes to Ocrl1 localization to ruffles. In fact, several proteins associated with clathrin-dependent pathways localize to membrane ruffles (33–38) and both AP2 and clathrin are present in these membrane structures (data not shown; Supplementary Material, Fig. S3A). We analyzed the ability of different GFP-Ocrl1 constructs to translocate to membrane ruffles in serum-stimulated HT1080 cells (Fig. 8B). Although all GFP-Ocrl1 versions (and also GFP-Inpp5b) showed a certain extent of ruffle localization,

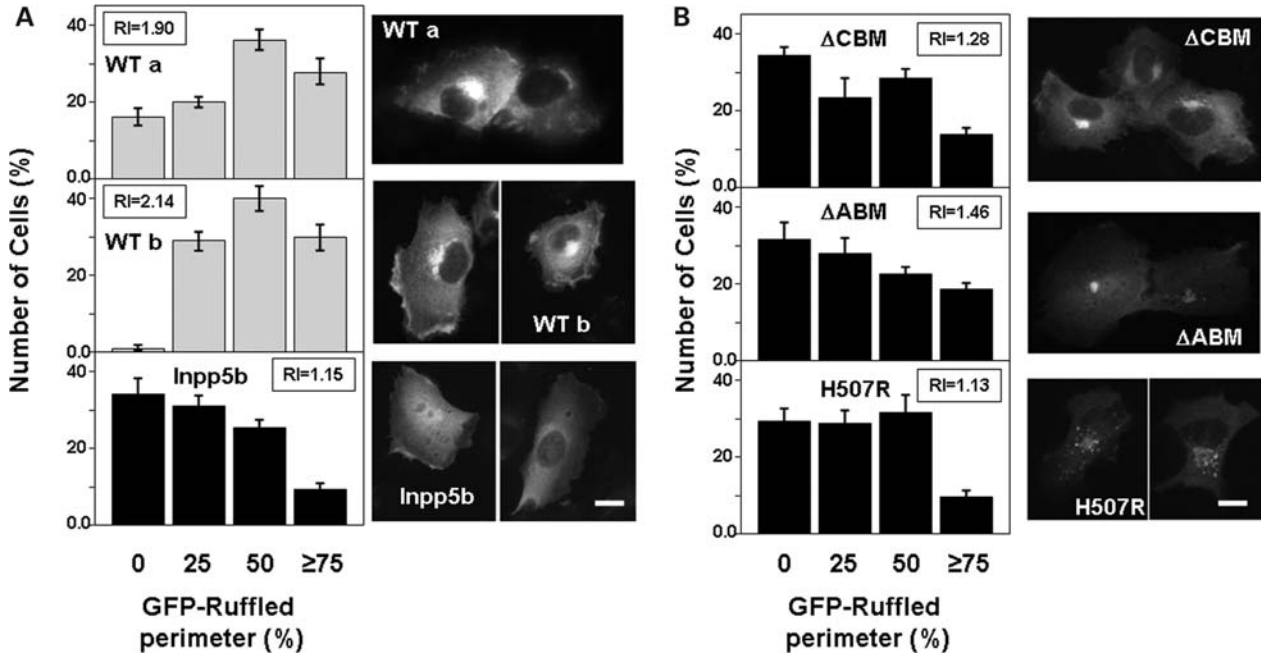

Figure 8. GFP-Ocrl1 lacking clathrin-/AP2-binding motifs or carrying non-functional phosphatase domain show decreased localization in membrane ruffles. (**A** and **B**) HT1080 cells expressing the indicated GFP-fusion proteins were starved for at least 8 h, stimulated for 15 min with 10% FBS, fixed and imaged. The number of cells displaying 0, 25, 50 or more than 75% of their perimeter decorated with ruffles positive for the corresponding GFP-fusion protein was determined. Values represent the mean ± SD of at least three independent determinations involving more than 100 cells randomly selected. Ruffling index (RI; see Materials and Methods) is also indicated. Representative images of each transfectant are included. Scale bars: 10 μm.

the Ocrl1 ΔCBM, ΔABM and H507R mutated proteins were markedly less abundant in these regions than WT Ocrl1 (Fig. 8A and B).

In agreement with a previous report (11), all Ocrl1 mutants displayed Golgi localization similar to WT Ocrl1 (Fig. 8B). Further, Ocrl1^{H507R}, which is deficient in phosphatase activity, appears to exhibit a fragmented pattern of Golgi localization. This observation agrees with those made using an Ocrl1 truncation that lacks the phosphatase domain (13). We also noted that in addition to its Golgi-localization, Ocrl1$^{\Delta ABM}$ displayed a broad, uniform plasma membrane distribution, as evidenced by its ability to mask nuclear visualization (Fig. 8B). This latter observation further supports our idea that binding to AP2 contributes to Ocrl1 localization at specific plasma membrane sites. We speculate that the Ocrl1 mutated proteins displayed a decrease in ruffle localization at the expense of enhanced Golgi/puncta (Ocrl1^{H507R} and Ocrl1$^{\Delta CBM}$) or homogenous plasma membrane (Ocrl1$^{\Delta ABM}$) distributions. These data support the hypothesis that clathrin and AP2 binding contribute to localization of Ocrl1 at membrane ruffles by a still-to-be-established mechanism perhaps shared with other clathrin-associated proteins (32–37).

Levels of expression of all GFP-fusion constructs were comparable (Supplementary Material, Fig. S2).

Ocrl1 also plays a role in cell spreading and fluid-phase uptake by human fibroblasts

We asked whether other membrane-intensive processes such as cell spreading (39) and fluid-phase uptake (40), are affected in LS cells. Therefore, the ability of freshly lifted cells to adhere and spread on fibronectin-coated surfaces was tested. Our results indicate that LS cells spread less than their normal counterparts (Fig. 9A). Moreover, LS cell populations were abundant in irregularly spread cells and enriched in early-spreading intermediates featuring actin-based microspikes (41) (Fig. 9B).

Membrane remodeling is also required for pinocytosis and fluid-phase uptake of extracellular material by cells (27,40). Although this process does not require clathrin, clathrin-associated and ruffle-localized proteins such as Dynamin-2 play a role in pinocytosis/fluid phase uptake (27). Therefore, we hypothesized that a deficiency in Ocrl1 could affect this process. Indeed, Figure 10A and B indicates that the uptake of TMR-labeled 70 kDa dextran was impaired in LS cells. Furthermore, knocking down Ocrl1, but not Inpp5b, in HeLa cells also decreased dextran uptake (Fig. 10B and C). Finally, we visualized GFP-Ocrl1 recruited to macropinosomal-derived structures filled with dextran (Supplementary Material, Fig. S4), supporting a role for Ocrl1 in fluid phase uptake.

DISCUSSION

This study reports the first LS cellular phenotype that is linked to the deficiency of Ocrl1 expression but independent of the functional status of the homologous phosphatase Inpp5b. Specifically, we found that fibroblasts from LS patients (which are deficient for Ocrl1 function) display abnormal cell migration, cell spreading and fluid-phase uptake. Therefore, and based on other investigators' and our own results, we propose that Ocrl1 displays functions that are (i) *shared*

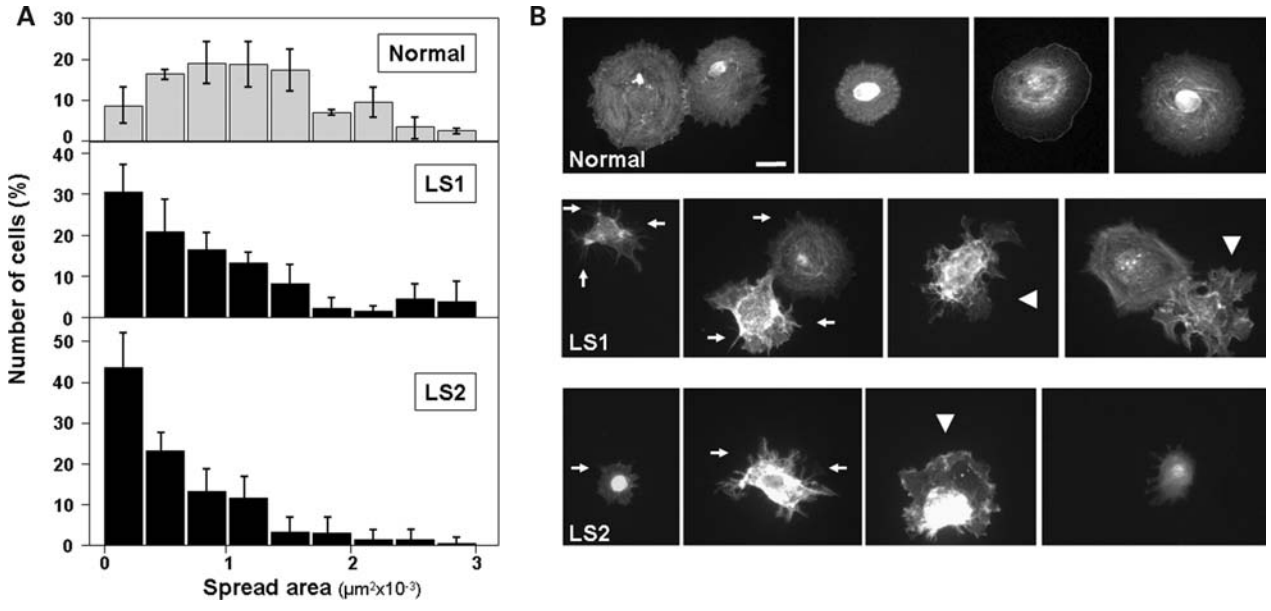

Figure 9. Dermal fibroblasts from LS patients show delays in cell spreading. (**A**) Normal and LS cells were resuspended and seeded on fibronectin-coated surfaces. After 30 min, the cells were fixed, stained with rhodamine–phalloidin and imaged. The area of at least 200 cells was computed using ImageJ software, the resulting size-distribution histograms are shown. (**B**) Examples of rhodamine–phalloidin-stained cells used for area-distribution determination (A) are shown for Normal and both LS patient cells. Arrows point to microspike structures typical of early spreading stages. Some irregularly spread cells are indicated by arrowheads. Scale bar: 20 μm.

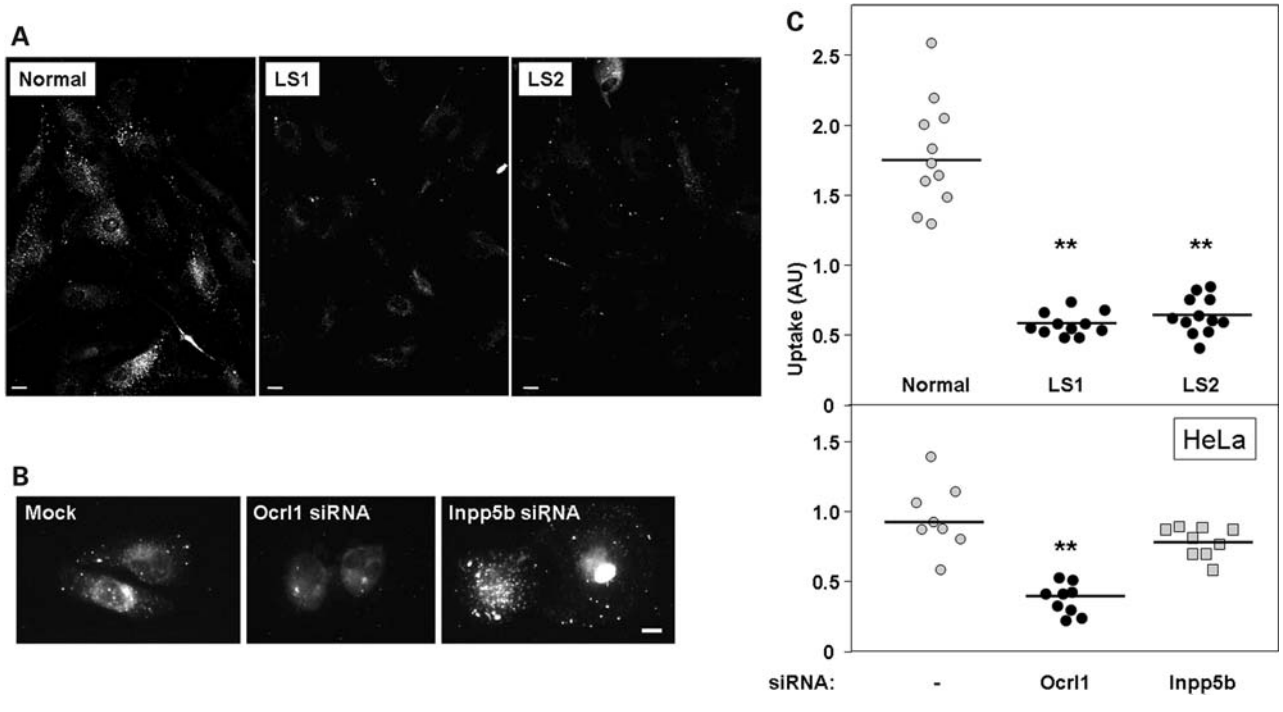

Figure 10. Dermal fibroblasts from LS patients display defects in fluid-phase uptake. (**A**) The amount of TMR-labeled 70 KDa dextran taken up by normal and LS patient cells was determined as described under Materials and Methods. After fixation cells were imaged using a rhodamine filter. Scale bar: 20 μm. (**B**). HeLa cells were mock-treated or subjected to siRNA-mediated knock-down of Ocrl1 or Inpp5b. After 72 h, cells were assayed for their ability to internalize TMR-dextran as described in (A). Scale bar: 10 μm. (**C**) TMR-labeled 70 KDa dextran uptake was quantified as described under Materials and Methods. Results from nine different experiments (involving 72–180 cells) are shown for indicated samples. The corresponding median is indicated by a horizontal line. Statistical significance of fluid-phase uptake phenotype with respect to control (Normal or Mock) was assessed by using the Wilcoxon test (**$P < 0.05$).

with the homologous phosphatase Inpp5b (22) and (ii) *Ocrl1-specific* (this work). Moreover, given the relevance of the processes involved we expect that deficiencies in Ocrl1-specifc functions will affect aspects of normal development and cell physiology.

Here we used different cell biological approaches to test the hypothesis that Ocrl1 is involved in cellular processes that rely on plasma membrane remodeling such as cell migration, spreading and fluid-phase uptake.

Our results indicate that fibroblasts from LS1 and LS2 patients and wild-type cells depleted of Ocrl1 are impaired for cell migration. This phenotype can be rescued by expression of $Ocrl1^{WT}$ (isoforms a and b), but not by introduction of a phosphatase-deficient version of Ocrl1 ($Ocrl1^{H507R}$) found in another LS patient (16) (Figs 2, 3 and 7).

We observed that LS1 and LS2 fibroblasts were impaired for cell migration even when they expressed significant levels of Inpp5b (Fig. 2A). Moreover, transfection of LS fibroblast with GFP-Inpp5b or Flag-Inpp5b did not rescue the defect in migration (Fig. 6A). Finally, knock-down of Ocrl1, but not of Inpp5b, reproduced the LS migration defect in HeLa cells (Fig. 6B). As a whole, our results indicate that the functional redundancy between Ocrl1 and Inpp5b does not extend to the role in cell migration of the former.

How does lack of Ocrl1 affect cell migration?

Ocrl1 is involved in vesicle trafficking (11–15,20). In fact, available evidence indicates that Ocrl1 is recruited to vesicular/tubular carriers that also contain cargo and clathrin (14; Supplementary Material, Movie S2 and Fig. S1). Since Ocrl1 binds key elements of the endocytosis machinery such as Rab GTPases, the AP2 and APPL1 adaptors and clathrin (11–15,20,21,42), Ocrl1 is predicted to play a role within the endocytic pathway. Our results suggest that lack of Ocrl1 does not affect receptor internalization (Supplementary Material, Fig. S3B), but do not rule out a post-internalization role by association with critical endosomal proteins like Rab5 and Appl1 (12,42). Whether these interactions play a role in cell migration/spreading/fluid-phase uptake remains to be elucidated and constitute the object of intense research in our laboratory.

Despite the abundant localization of Ocrl1 to the Golgi apparatus, we did not find evidence that LS cells exhibit major defects in Golgi apparatus polarization during cell migration. Instead, we observed that LS cells exhibit defects in other membrane ruffle-dependent processes, such as cell spreading and fluid-phase uptake (Figs 9 and 10). Further, our data support a role for the clathrin- and AP2-binding sites for Ocrl1 ability to sustain cell migration. However, we cannot ensure whether the AP2/clathrin binding requirement for Ocrl1 function obeys to a direct or indirect (e.g. by enhancing general Ocrl1 membrane recruitment) mechanism.

Although the mechanism by which the Ocrl1 interaction with clathrin/AP2 may contribute to ruffle function is unknown, several lines of evidence connect clathrin-dependent pathways with ruffle-related processes.

1. *Many proteins involved in clathrin-mediated endocytosis display functions in ruffle-mediated membrane remodeling*. Ocrl1 seems to be another member of a group of proteins (including amphiphysin1, SNX9, dynamin and myosin VI (33,35,36,43) that associate with clathrin structures and at the same time have membrane ruffle-dependent functions.

It is not clear how proteins that display clathrin-related functions participate in membrane remodeling processes. However, it is interesting to note that, in addition to AP2 and clathrin, Ocrl1 can interact with the ruffle formation-stimulating factors ARF6 (44) and Rac1 (45). Further, Ocrl1-deficient cells display abnormalities in the actin cytoskeleton (46), which in turn is central to ruffle formation.

2. *Interdependence between ruffle-mediated and clathrin-dependent pathways*. Our manuscript shows evidence that fluid-phase uptake is affected in Ocrl1-deficient cells (Fig. 10). Precedents found in the literature support the cross-talk between macropinocytosis/fluid phase uptake and clathrin-dependent endocytosis (47). For example, it is known that following macropinocytosis, there is a clathrin-dependent retrieval of cargo (48). In fact, we have also visualized Ocrl1 associated with macropinocytic structures (Supplementary Material, Fig. S3).

3. *Spatial coordination between clathrin and membrane remodeling pathways*. AP2 and clathrin have been observed polarized towards the ruffle-rich leading edge of migratory cells (29; Supplementary Material, Fig. S3). Likewise other regulatory/signaling proteins involved in ruffle dynamics, such as p600, are also found associated with clathrin and actin in regions of membrane extension (49). Furthermore, ARF6 is capable of both stimulating clathrin/AP2 membrane recruitment (50,51) and inducing ruffle formation (52). Finally, regions rich in the Ocrl1 substrate PIP_2 are known organizing centers for both endocytosis and membrane ruffling (53).

Therefore, although mechanistic details are unclear, data from multiple laboratories suggest that clathrin-dependent pathways and membrane remodeling processes can functionally intersect. Our data provide another example by showing that clathrin- and AP2-binding sites are required for Ocrl1-specific functions.

Why is the phosphatase activity of Ocrl1 required for cell migration?

The ruffled leading edge of migrating cells is a highly dynamic structure that depends on constant actin cytoskeleton rearrangements driven by the Rho GTPase Rac1 (54,55). Interestingly, PIP_2 is enriched in ruffles and is crucial for regulation of actin binding proteins (53,56) and possibly Rac1 recruitment to the plasma membrane (57).

Therefore, we believe that inositol phosphatases are key for the dynamic regulation of phospholipid levels. In fact, alteration of this PtdIns cycling by kinase overexpression (58) or by phosphatase deficiency (this work) interferes with cell migration. A similar effect was observed upon acute PIP_2 depletion (59), further reinforcing the relevance of PtdIns cycling. Since Ocrl1 is proposed to hydrolyze this lipid at membrane ruffles (9), we speculate that LS cells would exhibit deficiencies in their ability to promote the PIP_2 turnover necessary for leading edge dynamics.

What role do these Ocrl1-specific cellular phenotypes play in LS?

A conceptual breakthrough of LS pathology comes from the realization that target organs, such as brain and kidney, show low expression levels of Inpp5b (22). Thereby, in LS patients, deficiencies in Ocrl1 functions which are redundant with Inpp5b predict specific phenotypes associated with these organs (22).

Our findings indicate that there are also some Ocrl1 functions that cannot be fulfilled by Inpp5b. These include the role played by Ocrl1 in processes dependent on membrane remodeling such as cell migration, spreading and fluid-phase uptake.

The extent by which Ocrl1 functions will contribute to the clinical/phenotypic manifestations of Lowe Syndrome will depend on multiple variables and it is difficult to predict. These variables include the nature of the Ocrl1 mutation (truncation, functional hypomorph or no protein at all), genetic modifiers and genetic background, cell type, and tissue or extracellular matrix (ECM) properties (60).

In fact, cell migration and spreading are dramatically affected by the nature of the ECM and their importance varies depending on the cell type (61–63). Therefore, it is expected that upon Ocrl1 deficiency, some cell types in some organs or tissues will be more susceptible to display abnormalities in one versus another process (e.g. cell migration versus fluid-phase uptake phenotypes).

Nonetheless, we expect that the dramatic phenotypes displayed by LS cells will affect aspects of normal development and cell physiology. Hence, we believe that the findings reported in this work will contribute to refine the theoretical framework for understanding the molecular basis of LS and for shaping therapeutic efforts against this disease.

MATERIALS AND METHODS

Reagents

DAPI, Rhodamine-Phalloidin, FITC-transferrin and TMR-dextran were obtained from Invitrogen/Molecular probes. Other materials were purchased from Fisher Scientific (Fairlawn, NJ, USA) or Sigma (St Louis, MO, USA) unless noted otherwise.

Plasmids and antibodies

The following DNA constructions have been described previously: Ocrl1-GFP (14), Inpp5b-GFP, Flag-Inpp5b (32). mCherry-Clathrin light chain was a kind gift from M. Szczodrak and K. Rottner (Helmholtz Centre for Infection Research). Ocrl1 site-directed mutagenesis was performed using a QuikChange kit (Stratagene, La Jolla, CA, USA).

Preparation of sheep affinity purified antibodies against human Ocrl1 and rabbit affinity purified antibodies against human Inpp5b have been described previously (13,32). Other antibodies were obtained from commercial sources: mouse monoclonal anti-clathrin heavy chain X-22 (Affinity BioReagents), rabbit polyclonal anti-TGN46 (AbD), rabbit polyclonal anti-GFP (G1544, Sigma) and mouse monoclonal anti-α-tubulin DM1A (abcam).

Cells and cell culture

Normal and LS primary dermal fibroblasts (GM07492, GM 01676 and GM 03265) were obtained from the NIHGMS Human Genetic Cell Repository (Coriell Institute for Medical Research, Camden, NJ, USA). HT1080, HeLa and NIH3T3 cell lines were acquired from ATCC. Cells were cultured in DMEM, Streptomycin/Penicillin, 2 mM L-Glutamine and 15% (primary cells) or 10% (HT1080 and HeLa) fetal bovine serum (FBS), or 10% calf serum (NIH3T3). For experiments involving fibronectin-coated surfaces, bovine plasma fibronectin (Biomedical Technologies) was diluted in PBS and incubated on surfaces for 2 h at 37°C, washed twice with PBS and used.

Cell transfections

siRNA transfections. HeLa or NIH3T3 were seeded in 4 cm^2 cell culture plates and grown to 70% density in 24 h. Media was then exchanged for DMEM without serum and antibiotics 1 h before transfection. Cells were incubated 4 h with 4 μl Lipofectamine RNAiMax (Invitrogen) complexed with 40 pmoles of siRNA control (scrambled RNA, Santa Cruz: sc-37007), against Ocrl1 (Santa Cruz: sc-39073 for human and sc-39074 for mouse) or against human Inpp5b (M-021811, Dharmacon). The procedure was repeated twice, at 72 and 60 h before use. Complete media was added after 4 h each transfection.

siRNA/plasmid co-transfections. Cells prepared as above were incubated with 4 μl of DharmaFECT Duo (Dharmacon) complexed with 1 μg of plasmid DNA and 40 pmoles of siRNA. After 4 h, transfection media was replaced by complete media and cells were used 60–72 h later.

In all cases, we determined the viability of the knock-down with respect to the control cells by using a MTT assay (BioAssay Systems) (control: 100%; Ocrl1 knock-down: 98% and Inpp5b knock-down: 93%). The percentage of apoptotic and necrotic cells (apoptotic $\leq$0.5%; necrotic $\leq$2.0%) for all samples was also assessed using an Annexin-V-Fluos staining kit (Roche).

Plasmid transfections. HeLa, HT1080 and NIH3T3 cells were transfected by using *Trans* IT-LT1 (Mirus) according to manufacturer's instructions. Transfection of primary fibroblasts was achieved by electroporation as follows: approximately 1×10^6 cells from a subconfluent culture were trypsinized, washed with PBS and resuspended in 400 μl of ice-cold electroporation buffer (12 mM Hepes, 200 mM sucrose, 5 mM $MgCl_2$, 5 mM KH_2PO_4, 2 mM EDTA, 1% DMSO). Cell suspension was mixed with approximately 30 μg of plasmid DNA and transferred to a pre-chilled 0.2 cm electroporation cuvette and maintained at 4°C for 10 min. Cells were gently resuspended, pulsed at 400 V in a BioRad Gene Pulser and let rest on ice for 10 min. Cells were warmed up to 37°C and plated in complete media. Transfected cells were normally used 18–24 h after transfection.

SDS/PAGE and immunoblotting

Cell lysates in Laemmli's protein sample buffer were separated on 15-well 4–20% gradient gels (Pierce) at 20 mA constant current in SDS/PAGE running buffer (100 mM Tris base, 100 mM Hepes, 0.1% SDS) and transferred onto nitrocellulose membrane in transfer buffer (48 mM Tris, 1 mM SDS, 400 mM glycine,10% methanol) at 80 V for 90 min. Blots were blocked 1 h at room temperature in TBST-milk (25 mM Tris, 150 mM NaCl, 0.1% Tween-20, pH = 7.5, 5% non-fat dried milk) and incubated with the appropriate primary antibody and dilution (anti-Ocrl1:1:200; anti-Inpp5b: 1:500; anti-tubulin: 1:1000) overnight at 4°C or for 1 h at room temperature (anti-tubulin). After incubation with a secondary antibody conjugated with horseradish peroxidase for 1 h at room temperature and washing, specific bands were detected by chemiluminescence using SuperSignal West Femto (Pierce) as a substrate and visualized using a Alpha-Innotech imaging system (San Leandro, CA, USA). Densitometric analysis was carried out by using the corresponding tools from the imaging system software.

Cell staining and microscopy

In all cases, stained cells were imaged in a Zeiss Axiovert-200M microscope equipped with temperature-controlled, motorized stage for optical z-sectioning.

Immunofluorescence. Fixed cells were processed for immunofluorescence by incubating with primary antibodies in complete media containing 0.1% saponin for 60 min at room temperature. After washing with PBS, cells were incubated with secondary antibodies in media supplemented with saponin for 45 min. Coverslips were washed with PBS and mounted on slides using Aqua-PolyMount (Polysciences) and imaged.

DAPI and Rhodamine–phalloidin staining. DAPI stain was diluted to 1/20 000 in PBS and cells were stained for 20 min at room temperature. Rhodamine–phalloidin staining was conducted by incubating the cells with 30 nM rhodamine–phalloidin in media with 0.1% saponin for 45 min at room temperature.

Ruffling assays. Transfected HeLa and HT1080 cells grown on coverslips were incubated with starvation media (DMEM supplemented with 0.1% FBS) for 8–12 h followed by stimulation with 10% FBS for 15 min. Cells were then washed, fixed and the coverslips mounted on slides. The procedure for Ruffling Index (RI) determination was adapted from Cox *et al*. (64) to analyze migrating and spreading cells where ruffles are mostly located at the cell periphery. Briefly, more than 100 transfectants were randomly imaged at 40× magnification and the percentage of the cell perimeter that was decorated with ruffles containing GFP-fusion protein was determined. Cells were then individually scored using a scale of 0–3, where 0, no GFP-positive ruffles present, 1, 25%, 2, 50% and 3, ≥75% of cell perimeter covered with GFP-positive ruffles. A ruffling index was estimated as the sum of ruffling scores divided by the total number of cells scored.

Time-lapse microscopy. Cells were resuspended by trypsinization and allowed to recover in suspension for 1 h. Cells were then seeded in Lab-TekII #1.5 imaging chambers (Nalge Nunc) which were coated with fibronectin. Immediately before imaging, media was replaced with PBS containing appropriate amounts of serum and the chamber sealed and transferred to the temperature-controlled stage. Images were captured at 10 or 15 second intervals as indicated within 30 min after exchanging media for PBS.

Cell migration assays

Transwell cell migration assays. In the assay, 10^4 cells were trypsinized and trypsin quenched with complete media. Cells were then resuspended in 500 μl media containing 0.5% BSA and lacking FBS and allowed to recover in suspension for 1 h. Then cells were applied on 0.33 cm^2, 8 μm pore transwell inserts (Corning Inc) coated with 100 μg/ml BSA and 10 μg/ml fibronectin on the upper and bottom side of the insert membrane, respectively. Inserts were placed in wells containing media with 15% FBS and allowed to migrate for 6 h and fixed in 3% formaldehyde for 10 min. For cell migration experiments using established cell lines, migration times were modified to adapt to the higher migration rates of these cells (HeLa: 3 h; NIH3T3: 4 h). Cells on fixed membranes were stained with DAPI and visualized by epifluorescence microscopy. Total nuclei or transfected cells were counted per membrane in order to obtain cell inputs, then the upper side of the membrane was swabbed with a q-tip and rinsed with PBS. Cells on the bottom side of the membrane were visualized and scored as migrants if their nuclei passed through the membrane pores. Similar amounts of each type (control and Ocrl1- or Inpp5b-knock-down) were used in parallel assays. Migration results were normalized based on input values and expressed as the mean ± SD of triplicate membranes.

'Wound-healing' migration assays. A straight piece of a coverslip and a four-chamber Lab-TekII #1.5 imaging chamber (Nalge Nunc) were coated with 25 μg/ml fibronectin. Approximately 1×10^6 cells were trypsinized and the volume of cell suspension adjusted to 1.5 ml with complete media. After 1 h in suspension, cells were gently laid in the imaging chamber containing the coverslip and allowed to attach at 24°C for 30 min and spread at 37°C for 30 min. Then, unattached cells and coverslip were removed and 1.5 ml of fresh media was added. The chamber was sealed with parafilm and transferred to a heated-stage and the cell front was imaged under 10× magnification at 0 and 12 h.

Cell spreading assay

In the assay, 4.8 cm^2 coverslips were coated with 10 μg/ml fibronectin and blocked at 37°C for 30 min with 1% BSA. Cells were lifted with 20 mM EDTA in PBS, pelleted at 300 *g* for 5 min and resuspended in complete media. Cell suspensions were then added over fibronectin-coated coverslips and

allowed to spread for 30 min. After spreading, coverslips were gently rinsed with PBS and fixed in 3% formaldehyde for 10 min. Cells were stained with rhodamine–phalloidin and imaged by epifluorescence microscopy. Cell areas were traced and measured using ImageJ software.

Internalization assays

For internalization experiments, cells were seeded on glass coverslips for 12–36 h prior to experiments. For fluid-phase uptake experiments, cells were incubated with 1 mg/ml 70 kDa dextran-TMR in complete media containing FBS at 37°C for 20 min. Coverslips were cooled to 4°C in PBS and washed extensively for 5 min before fixation. For transferrin-FITC internalization experiments, cells were incubated for 12 h in starvation media (0.1% FBS). Coverslips were rinsed and chilled on ice before adding 1.25 ml/well of transferrin (3.0 μg/ml) in cold DMEM. Cells were transferred to 37°C for 10 min. Internalization was stopped by transferring the cells to ice and washing with ice-cold PBS. Non-internalized ligand was removed by washing with ice-cold 0.2N acetic acid containing 500 mM NaCl pH = 2.0 for 45 s. Cells were washed with ice-cold PBS, fixed and imaged by epifluorescence microscopy. Z-stack images of 8–10 random fields were captured at the same exposure times per experiment. Appropriate objectives were selected in order to both obtain multiple cells per field and yet resolve all endocytic structures. Approximately 15 cells per imaging field were obtained when imaging dextran-TMR uptake in human dermal fibroblasts and HeLa at 20× and 63× objectives, respectively, and about three cells per field were obtained when imaging transferrin-FITC uptake in human dermal fibroblasts with a 63× objective.

For image analysis, stacks were converted to single composite images. Background fluorescence was removed using the ImageJ's subtract background feature to remove continuously intense areas with a rolling ball radius of about 3.8 μm. Then images were despeckeled once to reduce additional noise. Specific fluorescence intensity per cell per field was calculated for several fields and used to quantify internalization.

SUPPLEMENTARY MATERIAL

Supplementary Material is available at *HMG* online.

ACKNOWLEDGEMENTS

We are indebted to Dr Robert Nussbaum (UCSF) for helpful discussions, suggestions and critical reading of the manuscript. We also thank Drs Chris Staiger and Henry Chang (Purdue University) for stimulating discussions and kindly providing reagents.

Conflict of Interest statement. None declared.

FUNDING

This work was possible thanks to a research grant (CA/PU/LSTJAN03) from the Lowe Syndrome Trust (UK) to R.C.A.

REFERENCES

1. Olivosglander, I.M., Janne, P.A. and Nussbaum, R.L. (1995) The Oculocerebrorenal syndrome gene-product is a 105-KD protein localized to the golgi-complex. *Am. J. Hum. Genet.*, **57**, 817–823.
2. Vicinanza, M., D'Angelo, G., Di Campli, A. and De Matteis, M.A. (2008) Phosphoinositides as regulators of membrane trafficking in health and disease. *Cell. Mol. Life Sci.*, **65**, 2833–2841.
3. Ooms, L.M., Horan, K.A., Rahman, P., Seaton, G., Gurung, R., Kethesparan, D.S. and Mitchell, C.A. (2009) The role of the inositol polyphosphate 5-phosphatases in cellular function and human disease. *Biochem. J.*, **419**, 29–49.
4. Attree, O., Olivos, I.M., Okabe, I., Bailey, L.C., Nelson, D.L., Lewis, R.A., McInnes, R.R. and Nussbaum, R.L. (1992) The Lowe's oculocerebrorenal syndrome gene encodes a protein highly homologous to inositol polyphosphate-5-phosphatase. *Nature*, **358**, 239–242.
5. Zhang, X.L., Jefferson, A.B., Auethavekiat, V. and Majerus, P.W. (1995) The protein-deficient in Lowe syndrome is a phosphatidylinositol-4,5-bisphosphate 5-phosphatase. *Proc. Natl Acad. Sci. USA*, **92**, 4853–4856.
6. Zhang, X.L., Hartz, P.A., Philip, E., Racusen, L.C. and Majerus, P.W. (1998) Cell lines from kidney proximal tubules of a patient with Lowe syndrome lack OCRL inositol polyphosphate 5-phosphatase and accumulate phosphatidylinositol 4,5-bisphosphate. *J. Biol. Chem.*, **273**, 1574–1582.
7. Di Paolo, G. and De Camilli, P. (2006) Phosphoinositides in cell regulation and membrane dynamics. *Nature*, **443**, 651–657.
8. Lin, T., Orrison, B.M., Suchy, S.F., Lewis, R.A. and Nussbaum, R.L. (1998) Mutations are not uniformly distributed throughout the OCRL1 gene in Lowe syndrome patients. *Mol. Genet. Metab.*, **64**, 58–61.
9. Faucherre, A., Desbois, P., Nagano, F., Satre, V., Lunardi, J., Gacon, G. and Dorseuil, O. (2005) Lowe syndrome protein Ocrl1 is translocated to membrane ruffles upon Rac GTPase activation: a new perspective on Lowe syndrome pathophysiology. *Hum. Mol. Genet.*, **14**, 1441–1448.
10. Dressman, M.A., Olivos-Glander, I.M., Nussbaum, R.L. and Suchy, S.F. (2000) Ocrl1, a Ptdlns(4,5)P-2 5-phosphatase, is localized to the trans-Golgi network of fibroblasts and epithelial cells. *J. Histochem. Cytochem.*, **48**, 179–189.
11. Choudhury, R., Noakes, C.J., McKenzie, E., Kox, C. and Lowe, M. (2009) Differential clathrin binding and subcellular localization of OCRL1 splice isoforms. *J. Biol. Chem.*, **284**, 9965–9973.
12. Erdmann, K.S., Mao, Y., McCrea, H.J., Zoncu, R., Lee, S., Paradise, S., Modregger, J., Biemesderfer, D., Toomre, D. and De Camilli, P. (2007) A role of the Lowe syndrome protein OCRL in early steps of the endocytic pathway. *Dev. Cell*, **13**, 377–390.
13. Choudhury, R., Diao, A.P., Zhang, F., Eisenberg, E., Saint-Pol, A., Williams, C., Konstantakopoulos, A., Lucocq, J., Johannes, L., Rabouille, C. *et al.* (2005) Lowe syndrome protein OCRL1 interacts with clathrin and regulates protein trafficking between endosomes and the trans-Golgi network. *Mol. Biol. Cell*, **16**, 3467–3479.
14. Ungewickell, A., Ward, M.E., Ungewickell, E. and Majerus, P.W. (2004) The inositol polyphosphate 5-phosphatase Ocrl associates with endosomes that are partially coated with clathrin. *Proc. Natl Acad. Sci. USA*, **101**, 13501–13506.
15. Hyvola, N., Diao, A., McKenzie, E., Skippen, A., Cockcroft, S. and Lowe, M. (2006) Membrane targeting and activation of the Lowe syndrome protein OCRL1 by rab GTPases. *EMBO J.*, **25**, 3750–3761.
16. Lin, T., Orrison, B.M., Leahey, A.M., Suchy, S.F., Bernard, D.J., Lewis, R.A. and Nussbaum, R.L. (1997) Spectrum of mutations in the OCRL1 gene in the Lowe oculocerebrorenal syndrome. *Am. J. Hum. Genet.*, **60**, 1384–1388.
17. Nobes, C.D. and Hall, A. (1999) Rho GTPases control polarity, protrusion, and adhesion during cell movement. *J. Cell Biol.*, **144**, 1235–1244.
18. Aznavoorian, S., Stracke, M.L., Parsons, J., McClanahan, J. and Liotta, L.A. (1996) Integrin alpha(v)beta(3), mediates chemotactic and haptotactic motility in human melanoma cells through different signaling pathways. *J. Biol. Chem.*, **271**, 3247–3254.
19. Eliceiri, B.P. (2001) Integrin and growth factor receptor crosstalk. *Circ. Res.*, **89**, 1104–1110.
20. Lowe, M. (2005) Structure and function of the Lowe syndrome protein OCRL1. *Traffic*, **6**, 711–719.

21. Fukuda, M., Kanno, E., Ishibashi, K. and Itoh, T. (2008) Large scale screening for novel Rab effectors reveals unexpected broad Rab binding specificity. *Mol. Cell. Proteomics*, **7**, 1031–1042.
22. Janne, P.A., Suchy, S.F., Bernard, D., MacDonald, M., Crawley, J., Grinberg, A., Wynshaw-Boris, A., Westphal, H. and Nussbaum, R.L. (1998) Functional overlap between murine Inpp5b and Ocrl1 may explain why deficiency of the murine ortholog for OCRL1 does not cause Lowe syndrome in mice. *J. Clin. Invest.*, **101**, 2042–2053.
23. Mao, Y., Balkin, D.M., Zoncu, R., Erdmann, K.S., Tomasini, L., Hu, F., Jin, M.M., Hodsdon, M.E. and De Camilli, P. (2009) A PH domain within OCRL bridges clathrin-mediated membrane trafficking to phosphoinositide metabolism. *EMBO J.*, **28**, 1831–1842.
24. Polo, S. and Di Fiore, P.P. (2006) Endocytosis conducts the cell signaling orchestra. *Cell*, **124**, 897–900.
25. Lanzetti, L. and Di Fiore, P.P. (2008) Endocytosis and Cancer: an 'Insider' Network with Dangerous Liaisons. *Traffic*, **9**, 2011–2021.
26. Palamidessi, A., Frittoli, E., Garre, M., Faretta, M., Mione, M., Testa, I., Diaspro, A., Lanzetti, L., Scita, G. and Di Fiore, P.P. (2008) Endocytic trafficking of Rac is required for the spatial restriction of signaling in cell migration. *Cell*, **134**, 135–147.
27. Schlunck, G., Damke, H., Kiosses, W.B., Rusk, N., Symons, M.H., Waterman-Storer, C.M., Schmid, S.L. and Schwartz, M.A. (2004) Modulation of Rac localization and function by dynamin. *Mol. Biol. Cell*, **15**, 256–267.
28. Schmid, E.M. and McMahon, H.T. (2007) Integrating molecular and network biology to decode endocytosis. *Nature*, **448**, 883–888.
29. Rappoport, J.Z. and Simon, S.M. (2003) Real-time analysis of clathrin-mediated endocytosis during cell migration. *J. Cell Sci.*, **116**, 847–855.
30. Nesterov, A., Carter, R.E., Sorkina, T., Gill, G.N. and Sorkin, A. (1999) Inhibition of the receptor-binding function of clathrin adaptor protein AP-2 by dominant-negative mutant mu 2 subunit and its effects on endocytosis. *EMBO J.*, **18**, 2489–2499.
31. Motley, A., Bright, N.A., Seaman, M.N.J. and Robinson, M.S. (2003) Clathrin-mediated endocytosis in AP-2-depleted cells. *J. Cell Biol.*, **162**, 909–918.
32. Williams, C., Choudhury, R., McKenzie, E. and Lowe, M. (2007) Targeting of the type II inositol polyphosphate 5-phosphatase INPP5B to the early secretory pathway. *J. Cell Sci.*, **120**, 3941–3951.
33. Yamada, H., Ohashi, E., Abe, T., Kusumi, N., Li, S.A., Yoshida, Y., Watanabe, M., Tomizawa, K., Kashiwakura, Y., Kumon, H. *et al.* (2007) Amphiphysin 1 is important for actin polymerization during phagocytosis. *Mol. Biol. Cell*, **18**, 4669–4680.
34. Yarar, D., Surka, M.C., Leonard, M.C. and Schmid, S.L. (2008) SNX9 activities are regulated by multiple phosphoinositides through both PX and BAR domains. *Traffic*, **9**, 133–146.
35. Lister, I., Roberts, R., Schmitz, S., Walker, M., Trinick, J., Veigel, C., Buss, F. and Kendrick-Jones, J. (2004) Myosin VI: a multifunctional motor. *Biochem. Soc. Trans.*, **32**, 685–688.
36. McNiven, M.A., Kim, L., Krueger, E.W., Orth, J.D., Cao, H. and Wong, T.W. (2000) Regulated interactions between dynamin and the actin-binding protein cortactin modulate cell shape. *J. Cell Biol.*, **151**, 187–198.
37. Cao, H., Orth, J.D., Chen, J., Weller, S.G., Heuser, J.E. and McNiven, M.A. (2003) Cortactin is a component of clathrin-coated pits and participates in receptor-mediated endocytosis. *Mol. Cell. Biol.*, **23**, 2162–2170.
38. Homayouni, R., Rice, D.S., Sheldon, M. and Curran, T. (1999) Disabled-1 binds to the cytoplasmic domain of amyloid precursor-like protein 1. *J. Neurosci.*, **19**, 7507–7515.
39. Herman, I.M., Crisona, N.J. and Pollard, T.D. (1981) Relation between between cell-activity and the distribution of cytoplasmic actin and myosin. *J. Cell Biol.*, **90**, 84–91.
40. Swanson, J.A. and Watts, C. (1995) Macropinocytosis. *Trends Cell Biol.*, **5**, 424–428.
41. Johnston, S.A., Bramble, J.P., Yeung, C.L., Mendes, P.M. and Machesky, L.M. (2008) Arp2/3 complex activity in filopodia of spreading cells. *BMC Cell Biol.*, **9**, 65–82.
42. McCrea, H.J., Paradise, S., Tomasini, L., Addis, M., Melis, M.A., De Matteis, M.A. and De Camilli, P. (2008) All known patient mutations in the ASH-RhoGAP domains of OCRL affect targeting and APPL1 binding. *Biochem. Biophys. Res. Commun.*, **369**, 493–499.
43. Yarar, D., Waterman-Storer, C.M. and Schmid, S.L. (2007) SNX9 couples actin assembly to phosphoinositide signals and is required for membrane remodeling during endocytosis. *Dev. Cell*, **13**, 43–56.
44. Lichter-Konecki, U., Farber, L.W., Cronin, J.S., Suchy, S.F. and Nussbaum, R.L. (2006) The effect of missense mutations in the RhoGAP-homology domain on ocrl1 function. *Mol. Genet. Metab.*, **89**, 121–128.
45. Faucherre, A., Desbois, P., Satre, V., Lunardi, J., Dorseuil, O. and Gacon, G. (2003) Lowe syndrome protein OCRL1 interacts with Rac GTPase in the trans-Golgi network. *Hum. Mol. Genet.*, **12**, 2449–2456.
46. Suchy, S.F. and Nussbaum, R.L. (2002) The deficiency of PIP2 5-phosphatase in Lowe syndrome affects actin polymerization. *Am. J. Hum. Genet.*, **71**, 1420–1427.
47. Donaldson, J.G., Porat-Shliom, N. and Cohen, L.A. (2009) Clathrin-independent endocytosis: A unique platform for cell signaling and PM remodeling. *Cell. Signal.*, **21**, 1–6.
48. Racoosin, E.L. and Swanson, J.A. (1993) Macropinosome maturation and fusion with tubular lysosomes in macrophages. *J. Cell Biol.*, **121**, 1011–1020.
49. Nakatani, Y., Konishi, H., Vassilev, A., Kurooka, H., Ishiguro, K., Sawada, J., Ikura, T., Korsmeyer, S.J., Qin, J. and Herlitz, A.M. (2005) p600, a unique protein required for membrane morphogenesis and cell survival. *Proc. Natl Acad. Sci. USA*, **102**, 15093–15098.
50. Krauss, M., Kinuta, M., Wenk, M.R., De Camilli, P., Takei, K. and Haucke, V. (2003) ARF6 stimulates clathrin/AP-2 recruitment to synaptic membranes by activating phosphatidylinositol phosphate kinase type I gamma. *J. Cell Biol.*, **162**, 113–124.
51. Zhang, Q., Calafat, J., Janssen, H. and Greenberg, S. (1999) ARF6 is required for growth factor- and Rac-mediated membrane ruffling in macrophages at a stage distal to Rac membrane targeting. *Mol. Cell. Biol.*, **19**, 8158–8168.
52. Poupart, M.E., Fessart, D., Cotton, M., Laporte, S.A. and Claing, A. (2007) ARF6 regulates angiotensin II type 1 receptor endocytosis by controlling the recruitment of AP-2 and clathrin. *Cell. Signal.*, **19**, 2370–2378.
53. Huang, S.H., Lifshitz, L., Patki-Kamath, V., Tuft, R., Fogarty, K. and Czech, M.P. (2004) Phosphatidylinositol-4,5-bisphosphate-rich plasma membrane patches organize active zones of endocytosis and ruffling in cultured adipocytes. *Mol. Cell. Biol.*, **24**, 9102–9123.
54. Hall, A. (1998) Rho GTPases and the actin cytoskeleton. *Science*, **279**, 509–514.
55. Mitchison, T.J. and Cramer, L.P. (1996) Actin-based cell motility and cell locomotion. *Cell*, **84**, 371–379.
56. Ling, K., Schill, N.J., Wagoner, M.P., Sun, Y. and Anderson, R.A. (2006) Movin' on up: the role of Ptdlns(4,5)P-2 in cell migration. *Trends Cell Biol.*, **16**, 276–284.
57. Yeung, T., Terebiznik, M., Yu, L.M., Silvius, J., Abidi, W.M., Philips, M., Levine, T., Kapus, A. and Grinstein, S. (2006) Receptor activation alters inner surface potential during phagocytosis. *Science*, **313**, 347–351.
58. Weinkove, D., Bastiani, M., Chessa, T.A.M., Joshi, D., Hauth, L., Cooke, F.T., Divecha, N. and Schuske, K. (2008) Overexpression of PPK-1, the Caenorhabditis elegans Type I PIP kinase, inhibits growth cone collapse in the developing nervous system and causes axonal degeneration in adults. *Dev. Biol.*, **313**, 384–397.
59. Zoncu, R., Perera, R.M., Sebastian, R., Nakatsu, F., Chen, H., Balla, T., Ayala, G., Toomre, D. and De Camilli, P.V. (2007) Loss of endocytic clathrin-coated pits upon acute depletion of phosphatidylinositol 4,5-bisphosphate. *Proc. Natl Acad. Sci. USA*, **104**, 3793–3798.
60. Genin, E., Feingold, J. and Clerget-Darpoux, F. (2008) Identifying modifier genes of monogenic disease: strategies and difficulties. *Hum. Genet.*, **124**, 357–368.
61. Georges, P.C. and Janmey, P.A. (2005) Cell type-specific response to growth on soft materials. *J. Appl. Physiol.*, **98**, 1547–1553.
62. Peyton, S.R., Ghajar, C.M., Khatiwala, C.B. and Putnam, A.J. (2007) The emergence of ECM mechanics and cytoskeletal tension as important regulators of cell function. *Cell Biochem. Biophys.*, **47**, 300–320.
63. von Dassow, M. and Davidson, L.A. (2007) Variation and robustness of the mechanics of gastrulation: the role of tissue mechanical properties during morphogenesis. *Birth Defects Res.*, **81**, 253–269.
64. Cox, D., Chang, P., Zhang, Q., Reddy, P.G., Bokoch, G.M. and Greenberg, S. (1997) Requirements for both Rac1 and Cdc42 in membrane ruffling and phagocytosis in leukocytes. *J. Exp. Med.*, **186**, 1487–1494.